J. Cent. South Univ. Technol. (2008) 15: 830−834
DOI: 10.1007/s11771−008−0153−1

Springer

Structure characterization and electrochemical properties of new lithium salt LiODFB for electrolyte of lithium ion batteries

GAO Hong-quan(高宏权), ZHANG Zhi-an(张治安), LAI Yan-qing(赖延清),
LI Jie(李 劼), LIU Ye-xiang(刘业翔)

(School of Metallurgical Science and Engineering, Central South University, Changsha 410083, China)

Abstract: Lithium difluoro(axalato)borate (LiODFB) was synthesized in dimethyl carbonate (DMC) solvent and purified by the method of solventing-out crystallization. The structure characterization of the purified LiODFB was performed by Fourier transform infrared (FTIR) spectrometry and nuclear magnetic resonance (NMR) spectrometry. The electrochemical properties of the cells using 1 mol/L $LiPF_6$ and 1 mol/L LiODFB in ethylene carbonate (EC)/DMC were investigated, respectively. The results indicate that LiODFB can be reduced at about 1.5 V and form a robust protective solid electrolyte interface (SEI) film on the graphite surface in the first cycle. The graphite/$LiNi_{1/3}Mn_{1/3}Co_{1/3}O_2$ cells with LiODFB-based electrolyte have very good capacity retention at 55 ℃, and show very good rate capability at 0.5*C* and 1*C* charge/discharge rate. Therefore, as a new salt, LiODFB is a most promising alternative lithium salt to replace $LiPF_6$ for lithium ion battery electrolytes in the future.

Key words: lithium ion battery; electrolyte; lithium difluoro(axalato)borate; synthesis; electrochemical properties

1 Introduction

Since the first commercialization of lithium ion batteries by Sony Corp. in 1991, lithium hexafluorophosphate ($LiPF_6$) remains the dominant salt of lithium ion battery. The commonly used $LiPF_6$ is sensitive to trace amount of moisture, resulting in by-products such as PF_5, POF_3, HF and LiF. In addition, $LiPF_6$ is of poor thermal stability. It starts to decompose at 40 ℃, and decomposes totally at 80 ℃. The side reactions of $LiPF_6$ make it difficult to meet the requirements of high energy density and long cycle life for hybrid electrical vehicle (HEV) application. Therefore, the development of a new alternative salt to replace $LiPF_6$ is attracting more and more attention now[1−4].

In 2006, ZHANG[5] reported the chemical structure of LiODFB (molecular formula: $LiBC_2O_4F_2$) that possesses the combined advantages of LiBOB and $LiBF_4$, and shows good electrochemical performances. He found that LiODFB could provide a high cycling efficiency for metallic lithium plating and stripping on the surface of Cu, and showed good passivation towards Al at high current rate. Recently, in high propylene carbonate (PC)-containing solutions, it is found that LiODFB used as electrolyte salt can provide stable SEI film and low cell impedance, which results in a dramatic improvement on both capacity retention and rate performance. Lithium ion batteries with LiODFB have excellent cycling performance even at 60 ℃[6−7]. Furthermore, it is found that the addition of small amount of LiODFB to the $LiPF_6$-based electrolyte can significantly improve both the capacity retention and the power retention of lithium ion batteries. But at the same time it will slightly increase the interfacial impedance of the cells[8−10]. So, thorough research on this salt needs to be done in order to get its widely commercial application.

In this work, LiODFB was synthesized and purified in dimethyl carbonate (DMC) solvent. And its structure was characterized and properties were analyzed. Then the synthesized LiODFB was dissolved in EC/DMC mixed solvents and used as electrolyte. The performance of cells using this lithium salt was also studied.

2 Experimental

2.1 Synthesis and structure characterization of LiODFB

$LiBF_4$(13.06 g) and anhydrous oxalic acid ($H_2C_2O_4$, 12.55 g) were dissolved in 500 mL DMC solvent, $SiCl_4$ was added drop-wise to the solution and stirred over night. The termination of the reaction was judged by confirming that gas generation stopped completely. DMC was evaporated on a RE-3000 rotary evaporator from Shanghai Yarong Company, China. The crude product

Foundation item: Project(2007BAE12B01) supported by the National Key Technology Research and Development Program of China; Project(20803095) supported by the National Natural Science Foundation of China
Received date: 2008−04−09; **Accepted date**: 2008−05−16
Corresponding author: ZHANG Zhi-an, PhD; Tel: +86−731−8876454; E-mail: zhianzhang@sina.com

was purified by the method of solventing-out crystallization[11−12]. The product yield was 80%.

^{13}C NMR, ^{11}B NMR and ^{19}F NMR spectra of the purified LiODFB were measured on a Bruker Avance 400 nuclear magnetic resonance spectrometer. And the structure characterization of the purified LiODFB was examined through a Nicolet Fourier transform infrared spectrometer (AVATAR360, USA).

2.2 Preparation of electrolyte and electrochemical performance measurement

$LiPF_6$ salt for application in batteries and EC and DMC solvents were purchased from Ferro Performance Materials Company. The LiODFB used was synthesized according to the method in Section 2.1.

The solvents were purified further through RE-3000 rotary evaporator and dried over 4A molecular sieve until the impurity contents were less than 0.005%. The water content was lower than 20×10^{-6}, as determined by Karl-Kisher titration (DL32, Switz). The acid content was lower than 2×10^{-6}, determined by Karl-Kisher titration (798 GPT Titrino, Switz). The base electrolytes used in this work, 1.0 mol/L $LiPF_6$ in EC/DMC solvents (mass ratio of EC to DMC is 1:1) and 1.0 mol/L LiODFB in EC/DMC solvents (mass ratio of EC to DMC is 1:1), respectively, were prepared in an Ar-filled glove box.

The half cells were assembled using Celgard 2400 as separator and an appropriate amount of electrolyte in an Ar-filled glove box. The working electrode was composed of 94% (mass fraction) graphite (G) and 6% PVDF binder. The counter and reference electrodes were lithium foils. The initial charge/discharge performance of Li/G half cells was evaluated using 2025 type coin cells on a Land charge/discharge instrument, China. The cells were cycled between 0 and 2.0 V at a constant current of 25.00 mA/g.

The full cells were assembled using Celgard 2400 as separator and an appropriate amount of electrolyte in an Ar-filled glove box. The positive electrode was composed of 84% (mass fraction) $LiNi_{1/3}Mn_{1/3}Co_{1/3}O_2$, 8% carbon black and 8% PVDF binder, and the negative electrode was composed of 94% (mass fraction) G and 6% PVDF binder. The initial charge-discharge performance of $G/LiNi_{1/3}Mn_{1/3}Co_{1/3}O_2$ cells was evaluated using 2025 type coin cells on a Land charge/discharge instrument, China. The charge cut-off and the discharge cut-off voltages were 4.2 and 2.5 V respectively at a constant current.

3 Results and discussion

3.1 Structure characterization of synthesized production

The FTIR test was employed to analyze functional groups of products synthesized. Fig.1 gives the comparison of the infrared spectra between the raw materials of $H_2C_2O_4$, $LiBF_4$ and the product of LiODFB. From Fig.1, it can be seen clearly that C═O stretching mode is at 1 687.17 cm^{-1} in the infrared spectrum of $H_2C_2O_4$. The strong absorption peak disappears here in the infrared spectrum of product, but two prominent feature peaks appear at 1 811.8 cm^{-1} and 1 764.95 cm^{-1}, which are probably assigned to C═O oscillating in phase and out of phase[13]. The absorption band observed at 1 370.74 cm^{-1} in the infrared spectrum of the product is assigned to the new formed B—O characteristic stretching vibration. Compared with the absorption peak of O—C—C stretching vibration at 1 252.86 cm^{-1} in the infrared spectrum of $H_2C_2O_4$, that of the same O—C—C stretching vibration shifts down to about 1 244.75 cm^{-1} due to appearance of B—O bond[13]. In the infrared spectra of $LiBF_4$ and LiODFB, the B—F asymmetric stretching vibration is typically near 1 636.74 cm^{-1}. In the infrared spectrum of $LiBF_4$, the broad twin peaks of F—B—F stretching vibration are at 1 082.27 and 1 034.71 cm^{-1}, while in the infrared spectrum of the product, and the broad peaks at 1 123.92 and 1 097.13 cm^{-1} are assigned to relative uncoupled O—B—O and F—B—F stretching vibration[14]. There is one medium-strong feature at 946.99 cm^{-1} identical to the wavenumber of B—O symmetric stretching mode in the infrared spectrum of the product. B—O deformation vibration also appears in the fingerprint region at 597.74 cm^{-1}[15]. The B—F asymmetric stretching mode cannot be seen here, most probably due to the overlapping with other nearby intense absorptions. From Fig.1, in addition to containing oxalate and B—F characteristic functional groups, there are O—B—O and F—B—F characteristic functional groups in structures of the product, which proves that the obtained product in this work is LiODFB.

This can be also certified by the NMR spectrum of the product. Fig.2 shows the ^{13}C NMR, ^{11}B NMR and ^{19}F NMR spectra of LiODFB. There is only one peak in

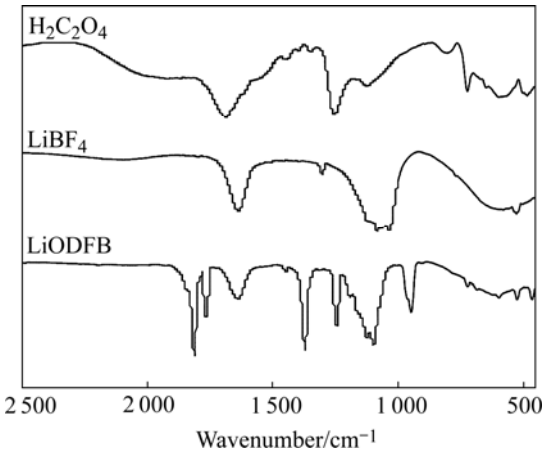

Fig.1 Infrared spectra of different samples

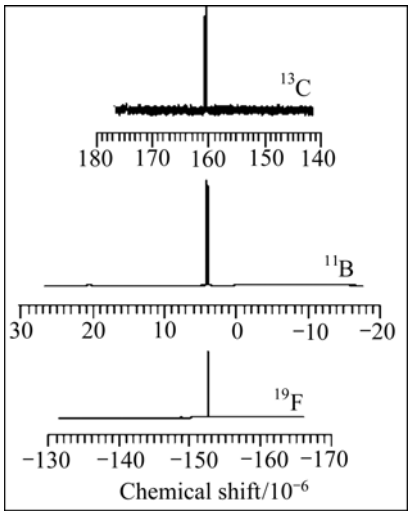

Fig.2 NMR spectrum of LiODFB

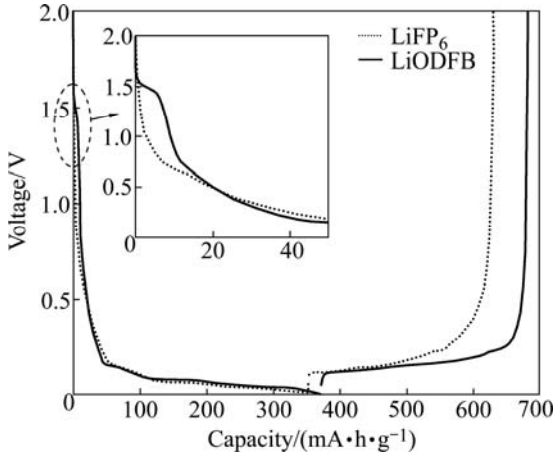

Fig.3 First charge/discharge profiles of graphite cells with different electrolytes at constant current

every spectrum due to the fact that the chemical states of the two C and two F atoms in the LiODFB molecule are the same. The chemical shift of ^{13}C is 160.5×10^{-6} (referenced to TMS in CD_3CN), the chemical shift of ^{11}B is 4.1×10^{-6} (referenced to $Et_2O{\cdot}BF_3$ in CD_3CN) and the chemical shift of ^{19}F is -152.6×10^{-6} (referenced to CCl_3F in CD_3CN), which was reported earlier in Ref.[11]. It can be concluded from the infrared spectra and the NMR spectra that fairly pure crystallization products have been obtained in this work.

3.2 First cycling performance of Li/G half cells

One of the unique properties of LiODFB is its excellent property in forming and stabilizing SEI film, which can effectively protect the negative electrode. Fig.3 shows the first charge/discharge profile of the graphite half cells using $LiPF_6$ salt and LiODFB salt, respectively. Compared with the cells using $LiPF_6$, the cells using LiODFB have larger discharge capacity and charge capacity, higher coulombic efficiency and smaller irreversible capacity. For the Li/G cell with $LiPF_6$ in EC/DMC, the charge and discharge capacities are 352.5 and 277.8 mA·h/g, respectively, and the coulombic efficiency of the first cycle is 78.8%. For the Li/G cell with LiODFB in EC/DMC, the charge and discharge capacities are 372.0 and 310.2 mA·h/g, respectively, and the coulombic efficiency of the first cycle is 83.4%. The improved performances are attributed to the better SEI film formed on the surface of graphite anode. Fig.3 shows that compared with $LiPF_6$-based electrolyte, a short potential reduction plateau is present at 1.5 V for LiODFB-based electrolyte (the inset is an enlargement of the selected part in Fig.3). One reason is that LiODFB undergoes reduction reactions that results in the formation of a preliminary SEI film. The other reason is that the presence of moisture and oxalate-related impurities can increase the length of irreversible 1.5 V plateau in the first cycle[16]. Because LiODFB can form and stabilize SEI film in the first cycle, LiODFB-based electrolyte exhibits a longer 0.2 V plateau of lithiation/delithiation, with better charge/discharge coulombic efficiency.

3.3 Rate performances of G/$LiNi_{1/3}Mn_{1/3}Co_{1/3}O_2$ cells

Fig.4 shows the electrochemical performances of the G/$LiNi_{1/3}Mn_{1/3}Co_{1/3}O_2$ cells using two different electrolytes at 0.5*C* and 1.0*C* discharge rate. The cell with $LiPF_6$-based electrolyte has higher initial discharge specific capacity (128.6 mA·h/g), while the initial discharge specific capacity of the cell with LiODFB-based electrolyte (117.6 mA·h/g) is much lower at 0.5*C* discharge rate. It is due to lower ionic conductivity of LiODFB-based electrolyte[17]. However, after 10 cycles, the discharge specific capacity of the cell with $LiPF_6$-based electrolyte (110.0 mA·h/g) is almost the same as that of the cell with LiODFB-based electrolyte (107.0 mA·h/g). The discharge specific capacity of the cell with $LiPF_6$-based electrolyte first increases, then decreases rapidly at 1.0*C* discharge rate. It may be because unstable SEI film formed by $LiPF_6$-based electrolyte results in the change of impedance of SEI film in cell. After 10 cycles, the discharge specific capacity is 100.7 mA·h/g, and the capacity retention is 78.3%. However, the discharge specific capacity of the cell with LiODFB-based electrolyte decreases and remains steady at 1.0*C* discharge rate. After 10 cycles, the discharge specific capacity is 94.1 mA·h/g, and the capacity retention is 80.0%. LiODFB-based electrolyte can maintain good cycling efficiency, which is attributed to stable SEI film formed on the surface of anode. Although LiODFB-based electrolyte has lower ionic

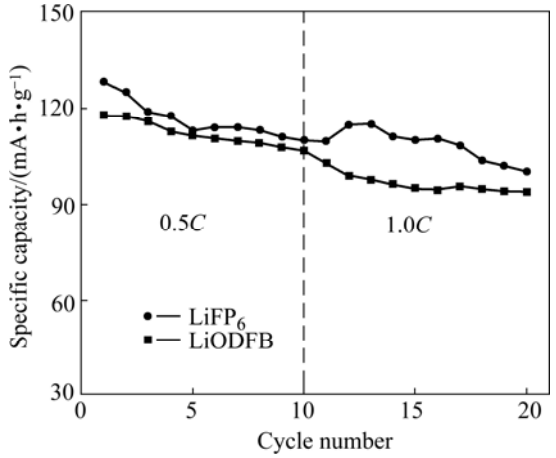

Fig.4 Cycling performances of G/$LiNi_{1/3}Mn_{1/3}Co_{1/3}O_2$ cells using different electrolytes at ambient temperature under various discharge rates

conductivity, it can form stable SEI films. The rate capability of the cell with the LiODFB-based electrolyte is almost as good as that of the cell with the $LiPF_6$-based electrolyte, and the gap between the two cells is tiny at 0.5*C* and 1 .0*C* discharge rates.

3.4 Elevated temperature cycling performances of G/ $LiNi_{1/3}Mn_{1/3}Co_{1/3}O_2$ cells

One of the unique properties of LiODFB is its excellent thermal stability. The cycling specific capacities of G/$LiNi_{1/3}Mn_{1/3}Co_{1/3}O_2$ cells at 55 ℃ and a constant current rate of 0.1*C* are shown in Fig.5. It shows that LiODFB-based electrolyte can improve cycling performance. When the $LiPF_6$-based electrolyte is used, the cell's initial capacity is 163.4 mA·h/g. After 100 cycles, the capacity retention is very low, only 69% at 55 ℃. When the LiODFB-based electrolyte is used, the cell's initial capacity is 132.8 mA·h/g. After 100 cycles, the capacity retention is about 92% at 55 ℃. Although the initial capacity of the cell using the LiODFB-based electrolyte is lower than that of the cell using the $LiPF_6$-based electrolyte, the irreversible capacity loss of the former is lower than that of the latter, and the capacity retention of the LiODFB-based electrolyte is much higher than that of the cell using the $LiPF_6$-based electrolyte. The improved cycling performances are attributed to the better SEI film formed on the surface of graphite anode at the first charge/ discharge cycle. The electrochemical performance of cells is remarkably affected by the structure and component of the SEI film. The SEI film formed in the electrolyte with $LiPF_6$ contains more inorganic components (such as Li_2CO_3 and LiF) that are less sensitive to temperature, while the SEI film formed in the electrolyte with LiODFB has more organic components that are more sensitive to temperature and has lower impedance at elevated temperature[10]. This is beneficial to remaining high capacity, reducing capacity loss of the cells and improving cycling performance of the cells.

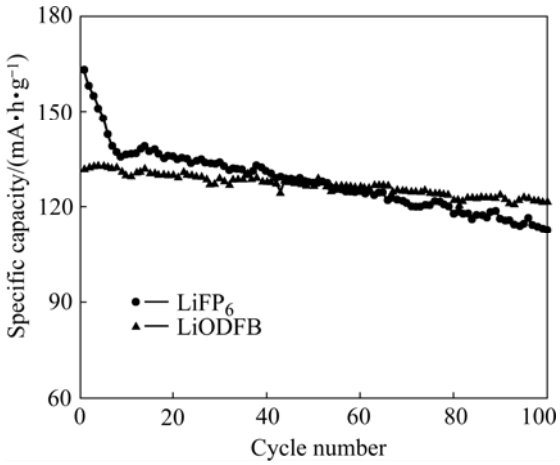

Fig.5 Cycling performances of G/$LiNi_{1/3}Mn_{1/3}Co_{1/3}O_2$ cells using different electrolytes at 0.1*C* rate and 55 ℃

Overall, LiODFB synthesized can maintain both high capacity retention and good rate performance in lithium ion battery. As a new salt, LiODFB is a most promising alternative salt for lithium ion battery electrolytes in the future.

4 Conclusions

1) LiODFB is synthesized in DMC, and purified by the method of solvent-out crystallization. Confirmed by the infrared spectrum and the NMR spectrum, the fairly pure crystallization products are obtained.

2) Compared with $LiPF_6$-based electrolyte, LiODFB-based electrolyte can form and stabilize SEI film on the surface of the graphite in the first cycle, the charge and discharge capacities of the Li/G using this electrolyte are 372.0 and 310.2 mA·h/g respectively and the initial coulombic efficiency of graphite is 83.4%.

3) At 0.5*C* and 1.0*C* discharge rates, the rate capability of the G/$LiNi_{1/3}Mn_{1/3}Co_{1/3}O_2$ cells with the LiODFB-based electrolyte is almost as good as that of the G/$LiNi_{1/3}Mn_{1/3}Co_{1/3}O_2$ cells with the $LiPF_6$-based electrolyte, and the gap between the two cells is tiny.

4) After 100 cycles, the capacity retention of the G/ G/$LiNi_{1/3}Mn_{1/3}Co_{1/3}O_2$ cells using LiODFB based electrolyte is about 92% at 55 ℃ and a constant current rate of 0.1*C*, and the cells using LiODFB-based electrolyte can maintain the higher capacity retention at the elevated temperature. Although LiODFB/EC+DMC electrolyte in G/$LiNi_{1/3}Mn_{1/3}Co_{1/3}O_2$ cells shows good electrochemical properties, the electrochemical performances of different electrode materials using this electrolyte still remain to be unclear. So much work still needs to be done.

References

[1] SASAKI Y, HANDA M, SEKIYA S, KATSUJI K, KYOHEI U. Application to lithium battery electrolyte of lithium chelate compound with boron [J]. Journal of Power Sources, 2001, 97/98: 561−565.

[2] SCHMIDT M, HEIDER U, KUEHNER A, OESTEN R, JUNGNITZ M, IGNAT'EV N, SARTORI P. Lithium fluoroalkylphosphates: A new class of conducting salts for electrolytes for high energy lithium-ion batteries [J]. Journal of Power Sources, 2001, 97/98: 557−560.

[3] ZHANG Sheng-shui. $LiBF_3Cl$ as an alternative salt for the electrolyte of Li-ion batteries [J]. Journal of Power Sources, 2008, 180(1): 586−590.

[4] HU Yong-jun, CHEN Bai-zhen, YUAN Yan. Preparation and electrochemical properties of polymer Li-ion battery reinforced by non-woven fabric [J]. Journal of Central South University of Technology, 2007, 14(1): 47−50.

[5] ZHANG Sheng-shui. An unique lithium salt for the improved electrolyte of Li-ion battery [J]. Electrochemistry Communications, 2006, 8(9): 1423−1428.

[6] ARAVINDAN V, VICKRAMAN P. A novel gel electrolyte with lithium difluoro(oxalato)borate salt and Sb_2O_3 nanoparticles for lithium ion batteries [J]. Solid State Sciences, 2007, 9(11): 1069−1073.

[7] ARAVINDAN V, VICKRAMAN P, KRISHNARAJ K. Lithium difluoro(oxalate)borate-based novel nanocomposite polymer electrolytes for lithium ion batteries [J]. Polymer International, 2008, 57(7): 932−938.

[8] ABRAHAM D P, FURCZON M M, KANG S H, DEES D W, JANSEN A N. Effect of electrolyte composition on initial cycling and impedance characteristics of lithium-ion cells [J]. Journal of Power Sources, 2008, 180(1): 612−620.

[9] ZHANG Sheng-shui. A review on electrolyte additives for lithium-ion batteries [J]. Journal of Power Sources, 2006, 162(2): 1379−1394.

[10] LIU J, CHEN Z H, BUSKING S, AMINE K. Lithium difluoro(oxalato)borate as a functional additive for lithium-ion batteries [J]. Electrochemistry Communications, 2007, 9(3): 475−479.

[11] HERZIG T, SCHREINER C, GERHARD D, WASSERSCHEID P, HEINER J G. Characterisation and properties of new ionic liquids with the difluoromono[1,2-oxalato(2-)-O,O′]borate anion [J]. Journal of Fluorine Chemistry, 2007, 128(6): 612−618.

[12] ZHANG Zhi-an, LAI Yan-qing, GONG Hong-quan, LI Fan-qun, LI Jie, YANG Juan, HAO Xin, LIU Ye-xiang. A purified method of lithium difluoro(axalato)borate: CN, 200810030568.2 [P]. 2008−01−30.

[13] ZHUANG G V, XU K, JOW T R, ROSS P N J. Study of SEI layer formed on graphite anodes in PC/LiBOB electrolyte using IR spectroscopy [J]. Electrochemical and Solid-State Letters, 2004, 7(8): A224−A227.

[14] ZHAO Yao-xing, SUN Xiang-yun. Identification of organic structure by spectrum [M]. Beijing: Science Press, 2003. (in Chinese)

[15] YU Bi-tao, QIU Wei-hua, LI Fu-shen, XU Guo-xiang. The electrochemical characterization of lithium bis(oxalato)borate synthesized by a novel method [J]. Electrochemical and Solid-State Letters, 2006, 9(1): A1−A4.

[16] ZHANG Sheng-shui. Electrochemical study of the formation of a solid electrolyte interface on graphite in a $LiBC_2O_4F_2$-based electrolyte [J]. Journal of Power Sources, 2007, 163(2): 713−718.

[17] CHEN Z H, LIU J, AMINE K. Lithium difluoro(oxalato)borate as salt for lithium-ion batteries [J]. Electrochemical and Solid-State Letters, 2007, 10(3): A45−A47.

(Edited by CHEN Wei-ping)